



# Computation of turbulent heat transfer in a moving porous bed using a macroscopic two-energy equation model<sup>☆</sup>

Marcelo J.S. de Lemos<sup>\*</sup>, Marcelo B. Saito

Departamento de Energia - IEME, Instituto Tecnológico de Aeronáutica - ITA, 12228-900 - São José dos Campos - SP - Brazil

## ARTICLE INFO

Available online 7 October 2008

**Keywords:**  
Turbulence  
Porous bed  
Moving bed  
Modeling

## ABSTRACT

Heat transfer between phases in a moving porous bed is analyzed. This work proposes a set of transport equations for solving problems involving turbulent flow and heat transfer in a moving bed equipment. The device is modeled as a saturated porous matrix in which the solid phase moves with a steady imposed velocity. Additional drag terms appearing the momentum equation, as well as interfacial heat transfer between phases, are assumed to be a function of the relative velocity between the fluid and solid phases. Turbulence transport equations are here also dependent on the speed of the solid material. Results indicate that, as the phases attain velocities of equal order, turbulence is damped and heat transfer between solid and fluid occurs mainly by conduction mechanism.

© 2008 Elsevier Ltd. All rights reserved.

## 1. Introduction

The use of biomass in modern combustion system has called the attention worldwide for its potential substitution of non-renewable fossil fuels. Biomass pelletization and preparation for energy production may consider systems having a moving porous bed [1–6]. The ability to realistic model such systems is of great advantage to a number of materials, food and energy production processes.

Accordingly, a turbulence model for flow in a fixed and rigid porous media has been proposed [7–9], which has been extended to non-buoyant heat transfer under local thermal equilibrium [10,11], buoyant flows [12–18], mass transfer [19] and double diffusion [20], including applications to channels with porous inserts [21] and baffles [22].

In addition, in an accompanying paper [23], movement of the solid phase in a porous bed was considered. However, in [23] only isothermal flow was treated. The purpose of this contribution is to extend the previous work on moving porous media [23], accounting now for the energy transfer between the fluid and the moving solid matrix.

## 2. Macroscopic model for fixed bed

A macroscopic form of the governing equations is obtained by taking the volumetric average of the entire equation set. In the development next, the porous medium is considered to be rigid, fixed and saturated by the incompressible fluid. As mentioned, derivation of this equation set is already available in the literature [7–9] so that details need not to be

repeated here. Nevertheless, for the sake of completeness, the final form of the modeled equations is here presented:

$$\nabla \cdot \bar{\mathbf{u}}_D = 0 \quad (1)$$

$$\rho \left[ \nabla \cdot \left( \frac{\bar{\mathbf{u}}_D \bar{\mathbf{u}}_D}{\phi} \right) \right] = -\nabla \left( \phi \langle \bar{p} \rangle^i \right) + \mu \nabla^2 \bar{\mathbf{u}}_D + \nabla \cdot \left( -\rho \phi \langle \bar{\mathbf{u}}' \bar{\mathbf{u}}' \rangle^i \right) - \left[ \frac{\mu \phi}{K} \bar{\mathbf{u}}_D + \frac{c_F \phi \rho |\bar{\mathbf{u}}_D| \bar{\mathbf{u}}_D}{\sqrt{K}} \right], \quad (2)$$

$$\rho \nabla \cdot \left( \bar{\mathbf{u}}_D \langle k \rangle^i \right) = \nabla \cdot \left[ \left( \mu + \frac{\mu_{t\phi}}{\sigma_k} \right) \nabla \left( \phi \langle k \rangle^i \right) \right] + P^i + G^i - \rho \phi \langle \varepsilon \rangle^i \quad (3)$$

$$\rho \nabla \cdot \left( \bar{\mathbf{u}}_D \langle \varepsilon \rangle^i \right) = \nabla \cdot \left[ \left( \mu + \frac{\mu_{t\phi}}{\sigma_\varepsilon} \right) \nabla \left( \phi \langle \varepsilon \rangle^i \right) \right] + c_1 P^i \frac{\langle \varepsilon \rangle^i}{\langle k \rangle^i} + c_2 \frac{\langle \varepsilon \rangle^i}{\langle k \rangle^i} \left( G^i - \rho \phi \langle \varepsilon \rangle^i \right) \quad (4)$$

where the  $c$ 's are constants,  $P^i = -\rho \langle \bar{\mathbf{u}}' \bar{\mathbf{u}}' \rangle^i : \nabla \bar{\mathbf{u}}_D$  is the production rate of  $\langle k \rangle^i$  due to gradients of  $\bar{\mathbf{u}}_D$  and  $G^i = c_k \rho \phi \langle k \rangle^i |\bar{\mathbf{u}}_D| / \sqrt{K}$  is the generation rate of the intrinsic average of  $k$  due to the action of the porous matrix.

For a fixed bed, temperatures for the fluid and solid phase are governed by,

$$(\rho c_p)_f \nabla \cdot \left( \bar{\mathbf{u}}_D \langle \bar{T}_f \rangle^i \right) = \nabla \cdot \left\{ \mathbf{K}_{\text{eff},f} \cdot \nabla \langle \bar{T}_f \rangle^i \right\} + h_i a_i \left( \langle \bar{T}_s \rangle^i - \langle \bar{T}_f \rangle^i \right) \quad (5)$$

$$0 = \nabla \cdot \left\{ \mathbf{K}_{\text{eff},s} \cdot \nabla \langle \bar{T}_s \rangle^i \right\} - h_i a_i \left( \langle \bar{T}_s \rangle^i - \langle \bar{T}_f \rangle^i \right) \quad (6)$$

<sup>☆</sup> Communicated by W.J. Minkowycz.

<sup>\*</sup> Corresponding author.

E-mail address: [delemos@ita.br](mailto:delemos@ita.br) (M.J.S. de Lemos).

**Nomenclature**

$c_F$	Forchheimer coefficient
$c's$	Constants in Eqs. (3) and (4)
$c_p$	Specific heat
$D$	Particle diameter, size of square rod.
$\mathbf{D}$	Deformation rate tensor, $\mathbf{D}=[\nabla\mathbf{u}+(\nabla\mathbf{u})^T]/2$
$G^i$	Production rate of $\langle k \rangle^i$ due to the porous matrix
$H$	Distance between channel walls
$k$	Turbulent kinetic energy per unit mass, thermal conductivity
$\langle k \rangle^v$	Volume (fluid + solid) average of $k$
$\langle k \rangle^i$	Intrinsic (fluid) average of $k$
$K$	Permeability
$L$	Channel length
$p$	Thermodynamic pressure
$\langle p \rangle^i$	Intrinsic (fluid) average of pressure $p$
$P^i$	Production rate of $k$ due to mean gradients of $\bar{\mathbf{u}}_D$ .
$Re$	Reynolds number
$\langle \bar{T}_f \rangle$	Averaged fluid temperature.
$\langle \bar{T}_s \rangle$	Averaged solid temperature.
$h_i$	Interfacial heat transfer coefficient
$\bar{\mathbf{u}}$	Microscopic time-averaged velocity vector
$\langle \bar{\mathbf{u}} \rangle^i$	Intrinsic (fluid) average of $\bar{\mathbf{u}}$
$\bar{\mathbf{u}}_D$	Darcy velocity vector, $\bar{\mathbf{u}}_D = \phi \langle \bar{\mathbf{u}} \rangle^i$
$\bar{\mathbf{u}}_{rel}$	Relative velocity based on total volume.

*Greek*

$\mu$	Fluid dynamic viscosity
$\mu_t$	Turbulent viscosity
$\mu_{t,b}$	Macroscopic turbulent viscosity
$\varepsilon$	Dissipation rate of $k$ , $\varepsilon = \mu \nabla u' : (\nabla u')^T / \rho$
$\langle \varepsilon \rangle^i$	Intrinsic (fluid) average of $\varepsilon$
$\rho$	Density
$\phi$	Porosity
$\gamma$	Phase identifier

*Subscript*

$s, f$	$s = \text{solid}, f = \text{fluid}$
--------	--------------------------------------

where  $\langle \bar{T}_f \rangle$ ,  $\langle \bar{T}_s \rangle^i$ ,  $\mathbf{K}'s$ ,  $h_i$  and  $a_i$  are the fluid and solid temperatures, the conductivity tensors, the interfacial heat transfer coefficient and the interfacial area per unit volume, respectively. The effective conductive tensors for the fluid and solid phases,  $\mathbf{K}_{eff,f}$  and  $\mathbf{K}_{eff,s}$ , respectively, account for all mechanisms contributing to the energy budget. A complete review of Eqs. (5) and (6) is beyond the scope of the present text and details of their derivation can be found in references [24–26].

**3. Interfacial heat transfer coefficient**

In Eqs. (5) and (6) the heat transferred between the two phases was modeled by means of a film coefficient,  $h_i$ , such that:

$$h_i a_i (\langle \bar{T}_s \rangle^i - \langle \bar{T}_f \rangle^i) = \frac{1}{\Delta V} \int_{A_i} \mathbf{n}_i \cdot k_f \nabla \bar{T}_f dA = \frac{1}{\Delta V} \int_{A_i} \mathbf{n}_i \cdot k_s \nabla \bar{T}_s dA. \quad (7)$$

where  $A_i$  is the interfacial area between the two phases and  $a_i$ , as mentioned above, is the interfacial area per unit volume or  $a_i = A_i / \Delta V$ . In foam-like or cellular media, the high values of  $a_i$  make them attractive for transferring thermal energy via conduction through the solid followed by convection to a fluid stream.

For numerically determining  $h_i$ , Kuwahara et al. (2001) [27] modeled a porous medium by considering it as an infinite number of solid square rods of size  $D$ , arranged in a regular triangular pattern. They numerically solved the governing equations in the void region, exploiting to advantage the fact that for an infinite and geometrically ordered medium a repetitive cell can be identified. Periodic boundary conditions were then applied for obtaining the temperature distribution under fully developed flow conditions. A numerical correlation for the interfacial convective heat transfer coefficient was then proposed by Kuwahara et al. (2001) [27] for laminar flow as:

$$\frac{h_i D}{k_f} = \left( 1 + \frac{4(1-\phi)}{\phi} \right) + \frac{1}{2} (1-\phi)^{1/2} Re_D Pr^{1/3}, \quad \text{valid for } 0.2 < \phi < 0.9, \quad (8)$$

Results in Eq. (8) depend on porosity and are valid for packed beds of particle diameter  $D$ . Saito and de Lemos (2005) [24] also obtained the interfacial heat transfer coefficient for laminar flows through an infinite square rod array using the same methodology as Kuwahara et al. (2001) [27]. For turbulent flow, Saito and de Lemos (2006) [25] extended the work in [24] for  $Re_D$  up to  $10^7$ . Both Low Reynolds and High Reynolds turbulence models were applied in [25]. The following expression was reviewed in de Lemos and Saito (2008) [26]:

$$\frac{h_i D}{k_f} = 0.08 \left( \frac{Re_D}{\phi} \right)^{0.8} Pr^{1/3}; \quad \text{for } 1.0 \times 10^4 < \frac{Re_D}{\phi} < 2.0 \times 10^7, \quad \text{valid for } 0.2 < \phi < 0.9, \quad (9)$$

Other correlations for determining interfacial heat transfer in fixed beds have been published (see for example Zhukauskas [28]).

**4. Macroscopic model for moving bed**

Here, only cases where the solid phase velocity is kept constant will be considered. A moving bed crosses a fixed control volume in addition to a flowing fluid, which is not necessarily moving with a velocity aligned with the solid phase velocity. The steps below show first some basic definitions prior to presenting a proposal for a set of transport equations for analyzing such systems.

A general form for a volume-average of any property  $\varphi$ , distributed within a phase  $\gamma$  that occupy volume  $\Delta V_\gamma$ , can be written as [29,30],

$$\langle \varphi \rangle^\gamma = \frac{1}{\Delta V_\gamma} \int_{\Delta V_\gamma} \varphi dV_\gamma \quad (10)$$

In the general case, the volume ratio occupied by phase  $\gamma$  will be  $\phi^\gamma = \Delta V_\gamma / \Delta V$ .

If there are two phases, a solid ( $\gamma=s$ ) and a fluid phase ( $\gamma=f$ ), volume average can be established on both regions. Also,

$$\phi^s = \Delta V_s / \Delta V = 1 - \Delta V_f / \Delta V = 1 - \phi^f \quad (11)$$

and for simplicity of notation one can drop the superscript “ $f$ ” to get  $\phi^s = 1 - \phi$ .

As such, calling the instantaneous local velocities for the solid and fluid phases,  $\mathbf{u}_s$  and  $\mathbf{u}$ , respectively, one can obtain the average for the solid velocity, within the solid phase, as follows,

$$\langle \mathbf{u} \rangle^s = \frac{1}{\Delta V_s} \int_{\Delta V_s} \mathbf{u}_s dV_s \quad (12)$$

which, in turn, can be related to an average velocity referent to the entire REV as,

$$\mathbf{u}_s = \frac{\overbrace{\Delta V_s}^{(1-\phi)}}{\Delta V} \frac{1}{\Delta V_s} \int_{\Delta V_s} \mathbf{u}_s dV_s = \frac{\Delta V_s}{\Delta V} \langle \mathbf{u} \rangle^s \quad (13)$$

A further approximation herein is that the porous bed is rigid and moves with a steady average velocity  $\mathbf{u}_s$ . Note that the condition of steadiness for the solid phase gives  $\mathbf{u}_s = \bar{\mathbf{u}}_s = \text{const}$  where the overbar denotes, as usual in the literature, time-averaging.

For the fluid phase, the intrinsic (fluid) volume average gives, after using the subscript “f” also for consistency with the literature,

$$\langle \bar{\mathbf{u}} \rangle^i = \frac{1}{\Delta V_f} \int_{\Delta V_f} \bar{\mathbf{u}} dV_f. \quad (14)$$

Both velocities can then be written as,

$$\bar{\mathbf{u}}_D = \phi \langle \bar{\mathbf{u}} \rangle^i, \quad \mathbf{u}_s = (1-\phi) \langle \mathbf{u} \rangle^s = \text{const}. \quad (15)$$

A total-volume based relative velocity is defined as,

$$\bar{\mathbf{u}}_{\text{rel}} = \bar{\mathbf{u}}_D - \mathbf{u}_s. \quad (16)$$

Incorporating now in Eq. (2) a model for the Macroscopic Reynolds Stresses  $-\rho \phi \langle \bar{\mathbf{u}}^i \bar{\mathbf{u}}^{i\prime} \rangle^i$  (see Ref. [7–26] for details), and assuming that a relative movement between the two phases is described by Eq. (16), the momentum equation reads,

$$\rho \left[ \nabla \cdot \left( \frac{\bar{\mathbf{u}}_D \bar{\mathbf{u}}_D}{\phi} \right) \right] - \nabla \cdot \left\{ (\mu + \mu_t) [\nabla \bar{\mathbf{u}}_D + (\nabla \bar{\mathbf{u}}_D)^T] \right\} = -\nabla \left( \phi \langle \bar{p} \rangle^i \right) - \frac{\mu \phi}{K} \bar{\mathbf{u}}_{\text{rel}} + \frac{c_F \phi \rho |\bar{\mathbf{u}}_{\text{rel}} \bar{\mathbf{u}}_{\text{rel}}}{\sqrt{K}}. \quad (17)$$

A corresponding transport equation for  $\langle k \rangle^i$  can be written as,

$$\rho \left[ \nabla \cdot \left( \bar{\mathbf{u}}_D \langle k \rangle^i \right) \right] = \nabla \cdot \left[ \left( \mu + \frac{\mu_t \phi}{\sigma_k} \right) \nabla \langle \phi \langle k \rangle^i \rangle \right] - \rho \langle \bar{u}^i \bar{u}^{i\prime} \rangle^i : \nabla \bar{\mathbf{u}}_D + \underbrace{c_k \rho \frac{\phi \langle k \rangle^i |\bar{\mathbf{u}}_{\text{rel}}|}{\sqrt{K}}}_{G^i} - \rho \phi \langle \varepsilon \rangle^i \quad (18)$$

where the generation rate due to the porous substrate,  $G^i$ , which was included in Eq. (3), now depends on  $|\bar{\mathbf{u}}_{\text{rel}}|$  and reads,

$$G^i = c_k \rho \phi \langle k \rangle^i |\bar{\mathbf{u}}_{\text{rel}}| / \sqrt{K}. \quad (19)$$

For analyzing moving beds, the energy equation for the fluid (Eq. (5)) remains the same, whereas convective transport is added to the solid-phase energy balance Eq. (6). A modeled form for then for a moving bed reads,

$$(\rho c_p)_f \nabla \cdot \left( \bar{\mathbf{u}}_D \langle \bar{T}_f \rangle^i \right) = \nabla \cdot \left\{ \mathbf{K}_{\text{eff},f} \cdot \nabla \langle \bar{T}_f \rangle^i \right\} + h_i a_i \left( \langle \bar{T}_s \rangle^i - \langle \bar{T}_f \rangle^i \right) \quad (20)$$

$$(\rho c_p)_s \nabla \cdot \left( \mathbf{u}_s \langle \bar{T}_s \rangle^i \right) = \nabla \cdot \left\{ \mathbf{K}_{\text{eff},s} \cdot \nabla \langle \bar{T}_s \rangle^i \right\} - h_i a_i \left( \langle \bar{T}_s \rangle^i - \langle \bar{T}_f \rangle^i \right). \quad (21)$$

The interstitial heat transfer coefficient  $h_i$  is also calculated by correlations (8) and (9) for laminar and turbulent flow, respectively. However, since the relative movement between phases is seen as the promoter of convective heat transport from the fluid to the solid, or vice-versa, a relative Reynolds number defined as,

$$\text{Re}_D = \frac{\rho |\bar{\mathbf{u}}_{\text{rel}}| D}{\mu} \quad (22)$$

is used in the correlations (8) and (9) instead of a Reynolds number based on the absolute velocity of the fluid phase. Accordingly, when the solid phase velocity approaches the fluid velocity, the only mechanism for transferring heat between phases is conduction.

## 5. Results and discussion

In order to apply the mathematical model proposed above, a numerical example is shown next. The flow under consideration is schematically presented in Fig. 1, where a channel is completely filled with a moving layer of a porous material. The channel shown in the figure has length and height given by  $L$  and  $H$ , respectively. The porous

matrix moves with constant velocity  $\mathbf{u}_s$  and its temperature at the entrance is kept constant and equal to  $T_{s,\text{in}}$ . A fluid flows longitudinally from left to right permeating through such moving porous structure with an inlet temperature  $T_{f,\text{in}}$ . The channel is kept insulated at north and bottom plates. Further, results at the channel center ( $y=H/2$ ) are a representative of uniform one-dimensional fully developed flow after a certain developing length. The numerical method applied was the Control Volume technique [31].

Temperature are plotted in terms of their non-dimensional value, defined as,

$$\Theta_{s,f} = \frac{T_{s,f} - T_{\text{min}}}{T_{\text{max}} - T_{\text{min}}} \quad (23)$$

where the subscripts  $s,f$  refers to the solid and fluid temperature, respectively. In addition, the maximum and minimum temperature are set as  $T_{s,\text{in}}$  and  $T_{f,\text{in}}$ , respectively.

### 5.1. Effect of Reynolds number, $\text{Re}_D$

Fig. 2 shows temperature along the centerline of the channel of Fig. 1 for different Reynolds number  $\text{Re}_D$  based on  $\bar{\mathbf{u}}_D$  and for a slip ratio  $(\mathbf{u}_s/\bar{\mathbf{u}}_D) = 0.5$ . As the inlet fluid velocity decreases, the fluid gets hotter and the temperature  $\Theta_f$  rises faster along the axial direction. Consequently, a lower drop in the solid temperature is obtained. On the other hand, the cooling effect of the hot porous material is well seen for a higher value of  $\text{Re}_D$ , when a greater reduction on the solid temperature occurs, mostly in the beginning of the channel. Final equilibrium temperature will then be reduced with increase of the mass flow rate through the bed.

### 5.2. Effect of porosity, $\phi$

The effect of porosity on longitudinal temperature distribution is shown in Fig. 3. The slip ratio  $\mathbf{u}_s/\bar{\mathbf{u}}_D$  and the Reynolds number are kept constant for all curves. The figure indicates that for a high porosity case, a smaller heat transfer area per unit volume, given by  $a_i = 4 \times (1-\phi)/D$  for a porous medium formed by square rods of size  $D$  (see Ref. [24–26]), decreases the total heat transfer rate from the solid material to the fluid. In such high porosity media, a longer developing length is needed for both materials to reach thermal equilibrium. Also, for a fixed Reynolds number based on  $\bar{\mathbf{u}}_D = \phi \langle \bar{\mathbf{u}} \rangle^i$ , an increase in  $\phi$  corresponds to a reduction on the fluid velocity  $\langle \bar{\mathbf{u}} \rangle^i$ , which further reduces the cooling effect by reducing the heat transfer coefficient  $h_i$  between phases. Consequently, the product  $h_i a_i$  in Eqs. (20) and (21) will be decreased as  $\phi$  increases, which, ultimately, indicates damping of convective transfer through the interfacial area.

### 5.3. Effect of slip ratio, $\mathbf{u}_s/\bar{\mathbf{u}}_D$

Fig. 4 shows values for the non-dimensional turbulent kinetic energy,  $\langle k \rangle^i / |\bar{\mathbf{u}}_D|^2$ , and for the non-dimensional temperatures,  $\Theta_f$  and  $\Theta_s$ , along the channel mid-height. As the relative phase velocity

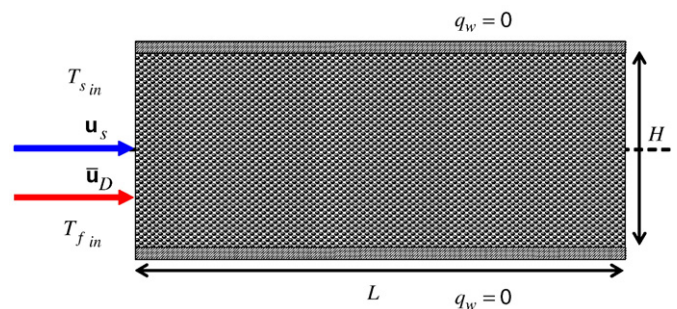


Fig. 1. Porous bed reactor with a moving solid matrix.

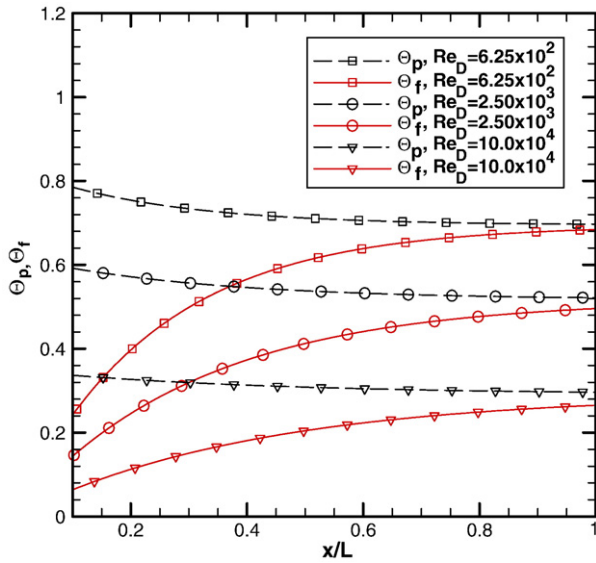


Fig. 2. Non-dimensional temperatures as a function of  $Re_D$  for  $u_s/\bar{u}_D=0.5$ ,  $\rho_s/\rho_f=10$ ,  $(\rho c_p)_s/(\rho c_p)_f=25$  and  $k_s/k_f=25$ .

decreases, the amount of fluid disturbance past the solid obstacles is reduced, implying then in a reduction of the final level of  $\langle k \rangle^i$ , according to  $G^*$  in Eq. (19) (Fig. 4a) [32]. Also, with an increase in  $u_s/\bar{u}_D$ , the solid carries more thermal energy by convection towards the inside of the reactor, raising the solid temperature for higher inlet solid velocity (Fig. 4b). The figure indicates that when the solid velocity approaches the fluid velocity, transfer of heat between phases tends to occur by a pure conduction mechanism, which requires a longer entry length for the two temperatures to achieve an equilibrium value. Finally, in Fig. 4c the raise of  $\Theta_f$  along the channel is presented. The figure seems to indicate that there is an optimum velocity ratio, above which the fluid temperature at the channel exit decreases. For the example here plotted, this optimal value is about  $u_s/\bar{u}_D \approx 0.75$ . This behavior could be explained by noting that the heat transfer between phases is proportional to  $h_i a_i \Delta T$ , as seen in Eqs. (20) and (21). Increasing  $u_s/\bar{u}_D$  raises  $\Theta_s$ , Fig. 4b, while reduces the product  $h_i a_i$  due to the use of a relative velocity to calculate  $Re_D$ , as shown in Eq. (22). Then, these two opposing trends will compete with each other as  $u_s/\bar{u}_D$  is varied, indicating the two-fold behavior of the curves in Fig. 4c.

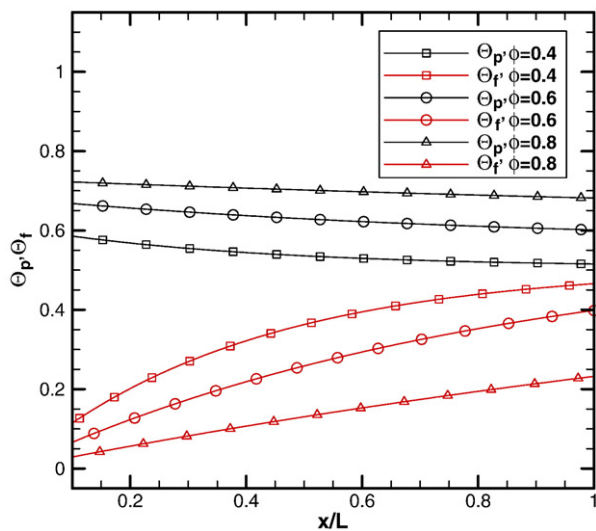


Fig. 3. Non-dimensional temperatures as a function of porosity  $\phi$  for  $u_s/\bar{u}_D=0.5$ ,  $\rho_s/\rho_f=10$ ,  $(\rho c_p)_s/(\rho c_p)_f=25$  and  $k_s/k_f=25$ .

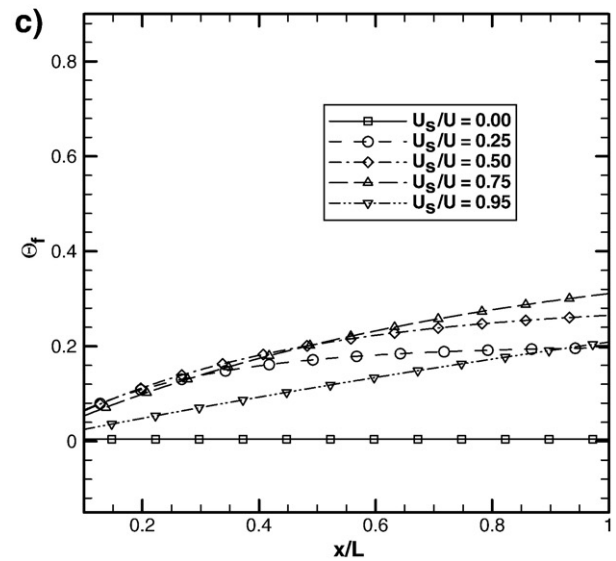
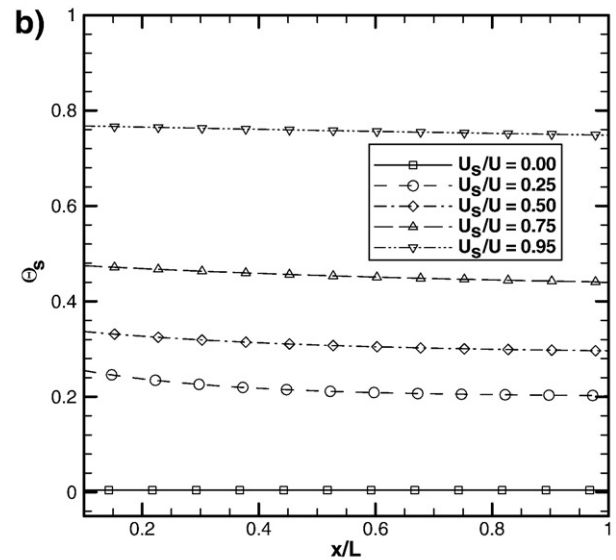
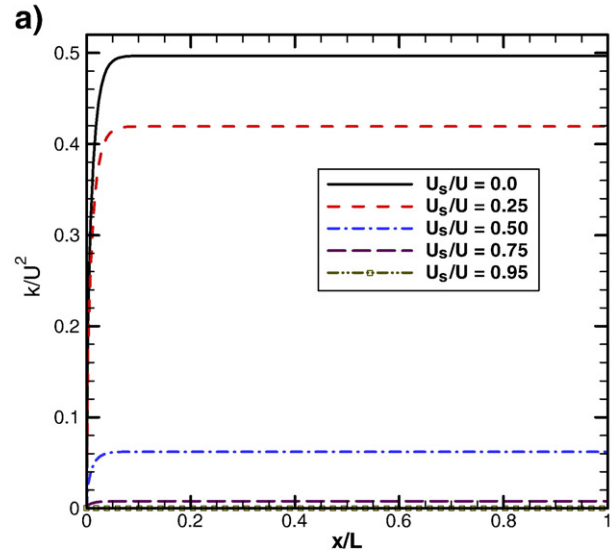


Fig. 4. Effect of  $u_s/\bar{u}_D$  for  $\phi=0.6$ : a)  $\langle k \rangle^i/\bar{u}_D^2$ ,  $Re_D=5 \times 10^4$ ; b) Solid temperature,  $\Theta_s$ ,  $Re_D=10^4$ ; c) Fluid temperature,  $\Theta_f$ ,  $Re_D=10^4$ .

## 6. Conclusions

Numerical solutions for turbulent flow in a moving porous bed were obtained for different ratios  $u_s/\bar{u}_D$ . Governing equations were discretized and numerically solved. Increasing the solid speed reduces the interfacial drag forces as well as the transfer of energy between phases, ultimately indicating that energy transport between phases mainly occurs due to conduction. Results herein may contribute to the design and analysis of engineering equipment where a moving porous body can be identified.

## Acknowledgments

The authors are thankful to CNPq and FAPESP, Brazil, for their invaluable support during the course of this research.

## References

- [1] Hu Guoxin, Xu Wei, Liu Yaqin, Heat transfer and gas flow through feed stream within horizontal pipe, *Transport in Porous Media* 52 (2003) 371–387.
- [2] R. Henda, D.J. Falcioni, Modeling of heat transfer in a moving packed bed: case of the preheater in nickel carbonyl process, *Journal of Applied Mechanics* 73 (2006) 47–53.
- [3] I.N.S. Winaya, T. Shimizu, Reduction of the volatile matter evolution rate from a plastic pellet during bubbling fluidized bed pyrolysis by using porous bed material, *Chemical Engineering & Technology* 30 (8) (2007) 1003–1009.
- [4] M.S. Valipour, Y. Saboohi, Modeling of multiple noncatalytic gas–solid reactions in a moving bed of porous pellets based on finite volume method, *Heat and Mass Transfer* 43 (9) (2007) 881–894.
- [5] T. Shimizu, J. Han, S. Choi, L. Kim, H. Kim, Fluidized-bed combustion characteristics of cedar pellets by using an alternative bed material, *Energy & Fuels* 20 (6) (2006) 2737–2742.
- [6] B. Gobel, U. Henriksen, T.K. Jensen, B. Qvale, N. Houbak, The development of a computer model for a fixed bed gasifier and its use for optimization and control, *Bioresource Technology* 98 (10) (2007) 2043–2052.
- [7] M.H.J. Pedras, M.J.S. de Lemos, Macroscopic turbulence modeling for incompressible flow through undeformable porous media, *International Journal of Heat and Mass Transfer* 44 (6) (2001) 1081–1093.
- [8] M.H.J. Pedras, M.J.S. de Lemos, Simulation of turbulent flow in porous media using a spatially periodic array and a low  $Re$  two-equation closure, *Numerical Heat Transfer - Part A* 39 (1) (2001) 35–59.
- [9] M.J.S. de Lemos, *Turbulence in Porous Media: Modeling and Applications*, Elsevier, Amsterdam, 2006.
- [10] F.D. Rocamora Jr, M.J.S. de Lemos, Analysis of convective heat transfer of turbulent flow in saturated porous media, *International Communications in Heat and Mass Transfer* 27 (6) (2000) 825–834.
- [11] M.J.S. de Lemos, F.D. Rocamora Jr, Turbulent transport modeling for heated flow in rigid porous media, *Proceedings of the Twelfth International Heat Transfer Conference*, Grenoble, France, August 18–23, 2002, pp. 791–795.
- [12] E.J. Braga, M.J.S. de Lemos, Turbulent natural convection in a porous square cavity computed with a macroscopic  $k-\epsilon$  model, *International Journal of Heat and Mass Transfer* 47 (26) (2004) 5639–5650.
- [13] E.J. Braga, M.J.S. de Lemos, Heat transfer in enclosures having a fixed amount of solid material simulated with heterogeneous and homogeneous models, *International Journal of Heat and Mass Transfer* 48 (23–24) (2005) 4748–4765.
- [14] E.J. Braga, M.J.S. de Lemos, Laminar natural convection in cavities filled with circular and square rods, *International Communications in Heat and Mass Transfer* 32 (10) (2005) 1289–1297.
- [15] E.J. Braga, M.J.S. de Lemos, Turbulent heat transfer in an enclosure with a horizontal porous plate in the middle, *Journal of Heat Transfer*, 128 (11) (2006) 1122–1129.
- [16] E.J. Braga, M.J.S. de Lemos, Simulation of turbulent natural convection in a porous cylindrical annulus using a macroscopic two-equation model, *International Journal of Heat and Mass Transfer* 49 (23–24) (2006) 4340–4351.
- [17] E.J. Braga, M.J.S. de Lemos, Computation of Turbulent Free Convection In Left And Right Tilted Porous Enclosures Using a Macroscopic  $k-\epsilon$  Model, *International Journal of Heat and Mass Transfer* 51 (21–22) (2008) 5279–5287.
- [18] E.J. Braga, M.J.S. de Lemos, Laminar and Turbulent Free Convection in a Composite Enclosure, *International Journal of Heat and Mass Transfer* (in press), doi:10.1016/j.ijheatmasstransfer.2008.07.012.
- [19] M.J.S. de Lemos, M.S. Mesquita, Turbulent mass transport in saturated rigid porous media, *International Communications in Heat and Mass Transfer* 30 (1) (2003) 105–113.
- [20] M.J.S. de Lemos, L.A. Tofaneli, Modeling of double-diffusive turbulent natural convection in porous media, *International Journal of Heat and Mass Transfer* 47 (19–20) (2004) 4221–4231.
- [21] M. Assato, M.H.J. Pedras, M.J.S. de Lemos, Numerical solution of turbulent channel flow past a backward-facing-step with a porous insert using linear and non-linear  $k-\epsilon$  models, *Journal of Porous Media* 8 (1) (2005) 13–29.
- [22] N.B. Santos, M.J.S. de Lemos, Flow and heat transfer in a parallel-plate channel with porous and solid baffles, *Numerical Heat Transfer Part A-Appl.* 49 (5) (2006) 471–494.
- [23] M.J.S. de Lemos, Turbulent kinetic energy in a moving porous bed, *International Communications in Heat and Mass Transfer* 35 (9) (2008) 1049–1052.
- [24] M.B. Saito, M.J.S. de Lemos, Interfacial heat transfer coefficient for non-equilibrium convective transport in porous media, *International Communications in Heat and Mass Transfer* 32 (5) (2005) 667–677.
- [25] M.B. Saito, M.J.S. de Lemos, A correlation for interfacial heat transfer coefficient for turbulent flow over an array of square rods, *Journal of Heat Transfer* 128 (2006) 444–452.
- [26] M.J.S. de Lemos, M.B. Saito, Interfacial heat transport in highly permeable media: a finite volume approach, in: A. Ochsner, G.E. Murch, M.J.S. de Lemos (Eds.), Chapter 1 in *Cellular and Porous Materials: Thermal Properties Simulation and Prediction*, WILEY-VCH Verlag, Weinheim, 2008.
- [27] F. Kuwahara, M. Shirota, A. Nakayama, A numerical study of interfacial convective heat transfer coefficient in two-energy equation model for convection in porous media, *International Journal of Heat and Mass Transfer* 44 (2001) 1153–1159.
- [28] A. Zhukauskas, *Heat transfer from tubes in cross flow*, *Advances in Heat Transfer*, vol. 8, Academic Press, New York, 1972.
- [29] W.G. Gray, P.C.Y. Lee, On the theorems for local volume averaging of multiphase system, *International Journal of Multiphase Flow* 3 (1977) 333–340.
- [30] S. Whitaker, *Advances in theory of fluid motion in porous media*, *Industrial and Engineering Chemistry* 61 (1969) 14–28.
- [31] S.V. Patankar, *Numerical Heat Transfer and Fluid Flow*, Hemisphere, New York, 1980.
- [32] M.J.S. de Lemos, Analysis of turbulent flows in fixed and moving permeable media, *Acta Geophysica* 56 (3) (2008) 562–583.